ELSEVIER

Materials Science and Engineering C 19 (2002) 9–13

MATERIALS SCIENCE & ENGINEERING C

www.elsevier.com/locate/msec

Catalyst traces and other impurities in chemically purified carbon nanotubes grown by CVD

L.P. Biró [a,*], N.Q. Khanh [a], Z. Vértesy [a], Z.E. Horváth [a], Z. Osváth [a], A. Koós [a], J. Gyulai [a], A. Kocsonya [b], Z. Kónya [c], X.B. Zhang [d], G. Van Tendeloo [d], A. Fonseca [e], J.B. Nagy [e]

[a] *Research Institute for Technical Physics and Materials Science, H-1525 Budapest, P.O. Box 49, Hungary*
[b] *KFKI Research Institute for Particle and Nuclear Physics, H-1525 Budapest, P.O. Box 49, Hungary*
[c] *Applied and Environmental Chemistry Department, University of Szeged, Rerrich Béla tér 1, H-6720, Szeged, Hungary*
[d] *EMAT-University of Antwerp (RUCA) Groenenborgerlaan 171, B-2020 Antwerp, Belgium*
[e] *Facultés Universitaires Notre-Dame de la Paix Rue de Bruxelles, 61 Namur, B-5000, Belgium*

Abstract

Multiwall carbon nanotubes grown by the catalytic decomposition of acetylene over supported Co catalyst were subjected to wet and dry oxidation in order to remove the unwanted products and the catalyst traces. The effects of the purification treatment on the Co content was monitored by physical methods: Rutherford Backscattering Spectrometry (RBS), Particle Induced X-Ray Emission (PIXE) and X-Ray Fluorescence (XRF). The purified products were investigated by microscopic methods: TEM, Scanning Electron Microscopy (SEM), Energy Dispersive Spectroscopy (EDS) and STM. The $KMnO_4/H_2SO_4$ aqueous oxidation procedure was found to be effective in reducing the Co content while damaging only moderately the outer wall of the nanotubes. Treatment in HNO_3/H_2SO_4 yields a bucky-paper like product and produces the increase of the Si and S content of the sample.

Keywords: Carbon nanotubes; Chemical purification; Impurities; Structural modification

1. Introduction

The discovery of carbon nanotubes a decade ago [1] marked the beginning of a new and very prolific research area bringing together scientist from the fields of nanostructures, fullerene science, physics, chemistry and materials science. The exciting properties of carbon nanotubes [2,3] and the wide range of the likely applications of these nano-objects ranging from nano-electronics to nano-electromechanical systems, fully justify the intense research interest that lead to the publication of several thousands of papers and several books on this topics.

Most of the widely used nanotube production methods: the arc method [4], the laser ablation [5], and the catalytic chemical vapor deposition (CVD) [6], are based on the use of transition metal catalysts. Following the production of carbon nanotube containing material, usually, some chemical purification method has to be used for removing the unwanted products like amorphous carbon, graphitic particles, catalyst traces, etc. The presence of impurities may influence the properties of the nanotubes and by this the behavior of any device built from this material. For practical applications of carbon nanotubes, the availability of analytic tools and methods for the rapid monitoring of the purification procedure and of the consequences of the purification on the structure of the nanotubes themselves is of paramount importance. In the present paper, we report on the use of Rutherford Backscattering Spectrometry (RBS), X-Ray Fluorescence (XRF), Particle Induced X-Ray Emission (PIXE), Scanning Electron Microscopy (SEM) and Energy Dispersive Spectroscopy (EDS), TEM and STM for the monitoring of the purification process and for the investigation of the modification induced by this process in the carbon nanotubes.

2. Experimental conditions

Carbon nanotubes were synthesized by the catalytic decomposition of acetylene as carbon source at 700 °C over zeolite supported cobalt-containing catalysts. For

* Corresponding author. Tel.: +36-1-2754993; fax: +36-1-3922226.
E-mail address: biro@mfa.kfki.hu (L.P. Biró).

0928-4931/02/$ - see front matter
PII: S0928-4931(01)00407-6

thicker tubes 2.5% Co (KZ50 and KZ60), for thinner tubes 2.5–2.5% Co–V mixture (KZ61) on faujasite type zeolites were used [7]. Separation of nanotubes and catalyst particles was carried out by repeated dissolution of the support in hydrofluoric acid and filtering. The zeolite-free nanotube samples were subjected to $KMnO_4/H_2SO_4$ aqueous oxidation procedure [8] in order to remove the amorphous carbon and graphitic particles. As an alternative to remove amorphous carbon, the catalyst-free material was oxidized in air. Oxidation in air was carried out at 400 °C, for 21 h (sample labeled "C"). For some samples, the first, wet oxidation was followed by soaking in a mixture of cc. HNO_3/H_2SO_4 (1:1 v/v) for 15 min applying ultrasonic mixing. After this, the reaction was carried out at 80 °C for 4 h followed by filtration, washing and drying at 120 °C overnight. The purification treatments applied to the different samples are detailed in Table 1. Increasing numerals after the dot in the sample name denote increasing number of treatments applied to samples from a certain family.

Nuclear analytical methods traditionally used in the semiconductor industry: RBS and PIXE were used in combination with XRF to monitor the changes of the Co content of several nanotube samples after the various chemical purification steps. A series of calibration samples prepared by ball milling of Co salts with active carbon were used to build calibration curves for RBS, XRF and PIXE.

The RBS measurements were carried out using 3550 keV $^4He^+$ ions with the scattering angle of 165° taking advantage of increase of about six times in the cross-section of He ion for carbon at this energy. Another benefit of using high energy ions is that the mass resolution for heavy elements is better than in the case of low energy ions. During the measurement, the vacuum in the scattering chamber was better than 1×10^{-4} Pa using liquid N_2 cooled traps along the beam path and around the wall of the chamber. Backscattered He ions were detected using an ORTEC surface barrier detector mounted in Cornell geometry. The RBX code [9] was used for the evaluation of the RBS spectra.

The RBS method is unable to separate the neighboring elements in the periodic system, especially the ones with larger atomic masses. Therefore, X-ray emission methods (XRF, PIXE) were used to determine the elemental composition of the samples. XRF is a simple and quick method to determine the average composition, practically no sample preparation is necessary. Its disadvantage is that requires relatively large amounts of samples (50–100 mg). A Cd-109 radioisotope induced X-ray spectrometer was used and the characteristic X-rays were detected by a Canberra 7333E detector. PIXE is a common method for trace element analysis of small amount of samples, with very low limits of detection ($\sim$1 ppm). The proton beam with energy of 2.5 MeV was produced by the 5 MV van de Graaff accelerator of KFKI RMKI. The X-ray detection system was the same, which had been used in the XRF measurements.

TEM and high resolution TEM (HRTEM) were used to investigate the modifications in the structure of the carbon nanotubes due to the purification treatment, and in an attempt to locate the catalyst particles present in the sample after the purification. HRTEM studies were performed in a Philips CM20 (Fig. 1a and b) and in a JEOL 200CX (Fig. 1c) microscope, both operating at 200 kV.

A JEOL JSM 840 SEM equipped with an Ortec System 5000 EDS was used to characterize the surface of the purified carbon nanotube material after washing, filtering and drying and to perform microanalysis.

The local electronic structure of the chemically treated carbon nanotubes was probed by a Nanoscope STM/AFM. The samples were prepared by sonicating the carbon nanotube containing material in toluene; droplets of the suspension were dispersed on HOPG and the solvent was left to evaporate. The topographic STM examination was carried out in ambient air using mechanically prepared PtIr tips, typical values of $I_t = 200$ pA and $U_b = 800$ mV were used.

3. Results and discussion

The steps of wet chemical purification applied to remove the amorphous carbon proved to be useful for the reduction of the catalyst content, too. The dry oxidation

Table 1
Wet chemical purification steps applied to the different nanotube samples

Sample	Zeolite removal in HF	$KMnO_4/H_2SO_4$ 0.3 equivalent $KMnO_4$	$KMnO_4/H_2SO_4$ 0.1 equivalent $KMnO_4$	HNO_3/H_2SO_4 (1:1 v/v)
KZ50.0	+	−	−	−
KZ50.1	+	+	−	−
KZ50.4	+	+	+	−
KZ60.0	+	+	−	−
KZ60.1	+	+	−	+
KZ61.0	+	+	−	−
KZ61.1	+	+	−	+

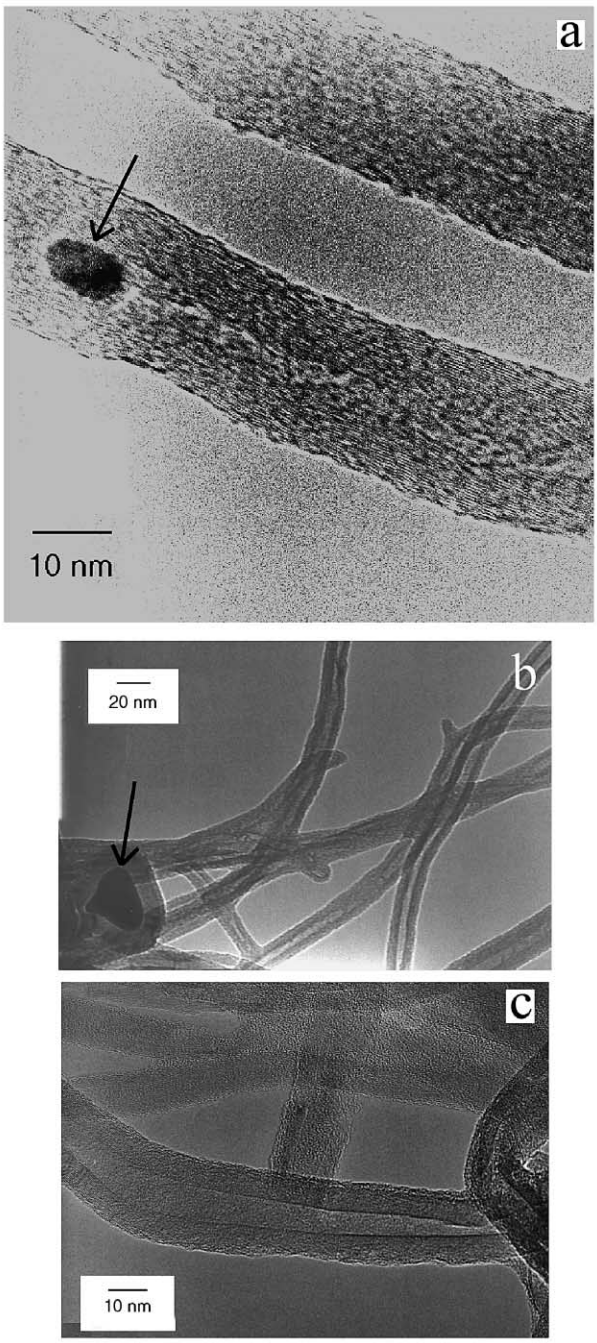

Fig. 1. TEM images of MWCNTs synthesized by the catalytic decomposition of acetylene using cobalt-containing catalysts. Co particles covered with graphitic carbon (in image b) and encapsulated in MWCNT (in image a) are denoted by arrows. (a) After repeated dissolution of the support in hydrofluoric acid and filtering (KZ50.0), (b) like (a), followed by two steps of aqueous oxidation in $KMnO_4/H_2SO_4$ solution, in the first step 0.3, while in the second step 0.1 equivalent $KMnO_4$ was used for the oxidation (KZ50.4), (c) like (a) and after dry oxidation in air ("C").

resulted in the increase of the relative Co content due to the reduction of the carbon content while the oxidized Co was not removed. The RBS, XRF and PIXE results are summarized in Table 2. One may remark that the Co concentration after the removal of the zeolite varies from sample to sample, in particular, the sample grown on Co–V catalyst (KZ61.0 and KZ61.1) has the lowest Co content. The low Co content in these samples is not compensated by V content; the EDS results did not evidenced V in these samples. The lower Co content of the KZ61 samples can be attributed to the smaller diameter of these tubes, which is associated with a smaller axial channel diameter. A significant fraction of the Co content is found as metallic particle inclusion in the axial hollows of the nanotubes (Fig. 1a). One may remark a systematic difference between the RBS and XRF data. The higher values of Co content given by RBS may be attributed to Fe impurity in the Co, these two elements have atomic masses too close to each other to be clearly separated by RBS even at the high ion energy used in the present measurements, while XRF and EDS can separate the two atomic species. As seen from Table 2, no chemical treatment, or combination of treatments, could completely eliminate the Co from the samples. Fig. 1b shows that even after two wet oxidation steps encapsulated metallic particles still can be found in the sample. These could be eliminated only after the complete destruction of the tubes. The dry oxidation of the carbon nanotubes produces a larger thickness of damaged region in the outer wall of the nantubes (Fig. 1c). Moreover, in the regions with numerous defects local "hollows" may be produced during dry oxidation [10].

STM investigation of the nanotube samples subjected to wet oxidation shows: the perfect nanotubes—these are usually straight bundles of few wall or single wall carbon nanotubes—are not damaged (Fig. 2), while the thicker and heavily curved tubes show a pronounced variation of the local electronic properties along the tube axis [10]. This is attributed to the attachment of functional groups to the defect rich regions on the outer wall of the nanotubes. In the case of wet oxidation treatment with $KMnO_4/H_2SO_4$, these functional groups are oxygen-containing groups (–OH, –COOH, –COOR and –COR) [11].

When the last wet purification treatment is done with HNO_3/H_2SO_4, a "bucky-paper" like product is obtained after washing, filtering and drying. As evidenced by SEM

Table 2
Co residue (weight percentage) in the different nanotube samples

Sample\ method	RBS (wt.%)	XRF (wt.%)	PIXE (wt.%)
KZ50.0	1.9	2.1	2.5
KZ50.1	1.6	1.1	0.9
KZ50.4	1.1	0.8	0.8
KZ60.0	2.5	1.6	–
KZ60.1	1.4	0.7	–
KZ61.0	0.8	0.3	–
KZ61.1	0.8	0.4	–
"C"	6.9	4.3	–

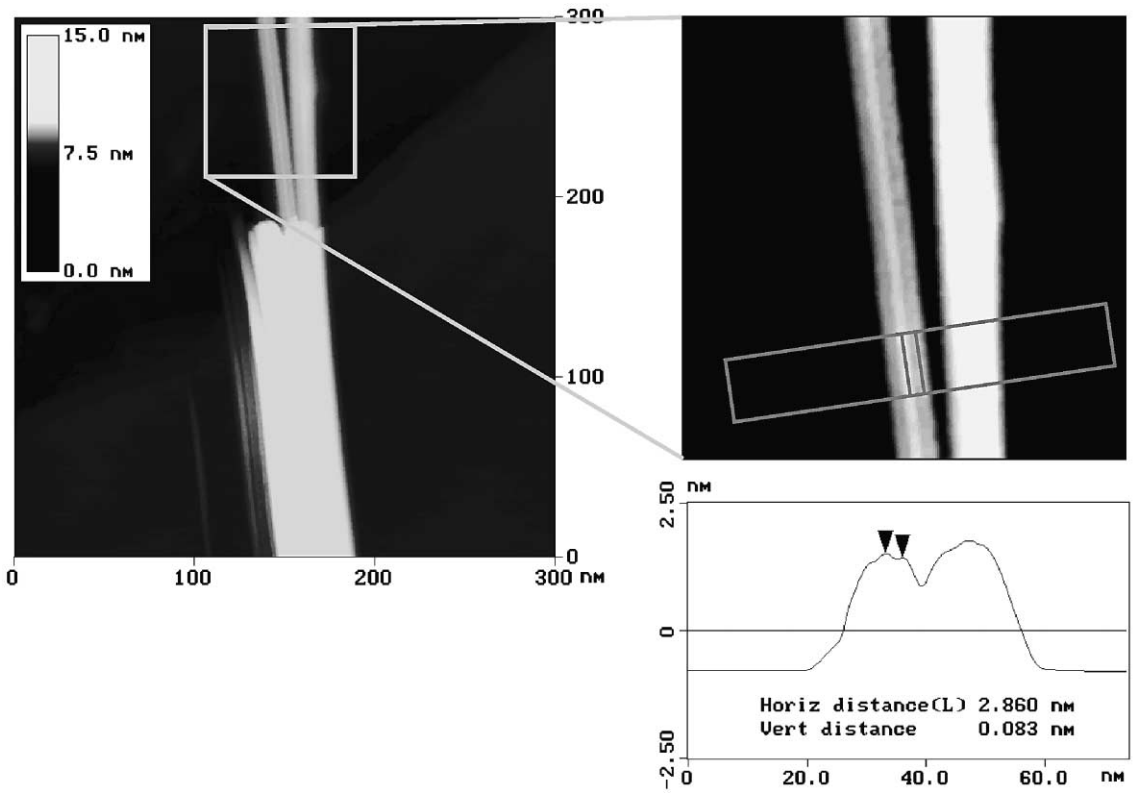

Fig. 2. Constant current STM image ($I_t = 200$ pA, $U_t = 800$ mV, Pt Ir tip) of a bundle catalytically grown single wall carbon nanotubes after two steps of wet oxidation. The uniformity of the gray shade along the individual tubes shows that the tubes were not attacked by the chemical treatment. The average line-cut taken in the rectangle marked on the right hand side detail shows a distance of 2.8 nm between the individual tubes building up the bundle.

examination, the two sides of this product have different topography and the Si impurity content, as measured by EDS, also shows some systematic differences (Table 3). The relative concentration values given by the EDS were converted to values of absolute concentration using the Co content as internal calibration standard. While the concentration of Co, Fe, and S does not show significant differences from one side of the bucky-paper to the other, both for KZ60 (Co catalyst) and for KZ61 (Co–V catalyst), the Si content of one side is 2 to 5 times higher. The HNO_3/H_2SO_4 treatment produces the increase of the S content to about 0.3–0.4 wt.%. This may be attributed to the attachment of S containing functional groups. Further investigations are needed to decide which functional group is responsible for the formation of the bucky-paper structure.

4. Conclusions

Catalitically grown carbon nanotubes were subjected to wet and dry chemical purification for the removal of unwanted carbonaceous products and of the catalyst particles. Wet oxidation is effective in achieving both goals and produces a relatively moderate damage of the outer wall of the nanotubes. Various physical analytical methods: RBS, PIXE, XRF, TEM, HRTEM, SEM, EDS and STM were

Table 3
EDS concentration values of Si, S and Fe

Element	Concentration (wt.%) KZ60.0	Concentration (wt.%) KZ60.1 Side C	Concentration (wt.%) KZ60.1 Side D	Concentration (wt.%) KZ61.0	Concentration (wt.%) KZ61.1 Side A	Concentration (wt.%) KZ61.1 Side B
Si	0.08	1.24	2.30	0.56	1.09	0.20
S	0.01	0.27	0.30	0.15	0.40	0.39
Fe	0.48	0.16	0.12	0.13	0.12	0.12
Co	1.6	0.7	0.7	0.3	0.4	0.4

Relative values were converted to absolute values using the Co concentration measured by XRF (Table 1).

used to investigate the material resulted after the purification. RBS, PIXE and XRF were found to be equally suitable for monitoring the changes in the Co catalyst content, however, RBS may be unsuitable if mixed transition metal catalyst are used.

The catalyst particles encapsulated in the central channel of the carbon nanotubes cannot be removed even if repeated treatments are applied. STM measurements show that the outer surface of the thin, defect-free carbon nanotubes is not damaged by the wet oxidation, while the tubes containing numerous defects are selectively attacked in the defect rich regions.

The HNO_3/H_2SO_4 treatment produces the functionalization of the outer surface of nanotubes with S containing groups and causes a nonuniform Si buildup in the bucky-paper like product.

Acknowledgements

This work was supported by the EU5, contracts NANOCOMP, HPRN-CT-2000-00037 and EU5 Centre of Excellence ICAI-CT-2000-70029, and by OTKA grants T 30435 and T 25928 in Hungary. LPB, ZV, and ZEH gratefully acknowledge grants from the Belgian FNRS and KVABWK, respectively.

References

[1] S. Iijima, Nature (London) 354 (1991) 56.
[2] M.S. Dresselhaus, G. Dresselhaus, P.C. Ecklund, Science of Fullerenes and Carbon Nanotubes, Academic Press, San Diego, 1996.
[3] L.P. Biró, C.A. Bernardo, G.G. Tibbets, Ph. Lambin (Eds.), Carbon Filaments and Carbon Nanotubes: Common Origins, Differing Applications? Kluwer Academic Publishing, Dordrecht, 2001.
[4] C. Journet, W.K. Maser, P. Bernier, A. Loiseau, M. Lamy de la Chapelle, S. Lefrant, P. Deniard, R. Lee, J.E. Fisher, Nature 388 (1997) 756.
[5] A. Thess, R. Lee, P. Nikolaev, P. Dai, P. Petit, J. Robert, C. Xu, Y.H. Lee, S.G. Kim, A.G. Rinzler, D.T. Colbert, G.E. Scuseria, D. Tomanek, J.E. Fisher, R.E. Smalley, Science 273 (1996) 483.
[6] V. Ivanov, J.B. Nagy, Ph. Lambin, A. Lucas, X.B. Zhang, X.F. Zhang, D. Bernaerts, G. Van Tedeloo, S. Amelinckx, J. Van Landuyt, Chem. Phys. Lett. 223 (1994) 329.
[7] I. Willems, Z. Konya, J.-F. Colomer, G. Van Tendeloo, N. Nagaraju, A. Fonseca, J.B. Nagy, Chem. Phys. Lett. 317 (2000) 71.
[8] J.-F. Colomer, P. Piedigrosso, I. Willems, C. Journet, P. Bernier, G. Van Tendeloo, A. Fonseca, J.B. Nagy, J. Chem. Soc., Faraday Trans. 94 (1998) 3753.
[9] E. Kótai, Nucl. Instrum. Methods B 85 (1994) 588.
[10] L.P. Biró, N.Q. Khanh, Z.E. Horváth, Z. Vértesy, A. Kocsonya, Z. Kónya, Z. Osváth, A.A. Koós, J. Gyulai, X.B. Zhang, G. Van Tendeloo, A. Fonseca, J.B. Nagy, Kirchberg, 2001, in press.
[11] J.B. Nagy, A. Fonseca, N. Pierard, I. Willems, G. Bister, C. Pirlot, J. Delhalle, Z. Mekhalif, K. Niesz, Ch. Bossuot, J.-P. Pirard, L.P. Biró, Z. Kónya, J.-F. Colomer, G. Van Tendeloo, I. Kiricsi, Kirchberg, 2001, in press.